SUPPLEMENTARY FIGURES

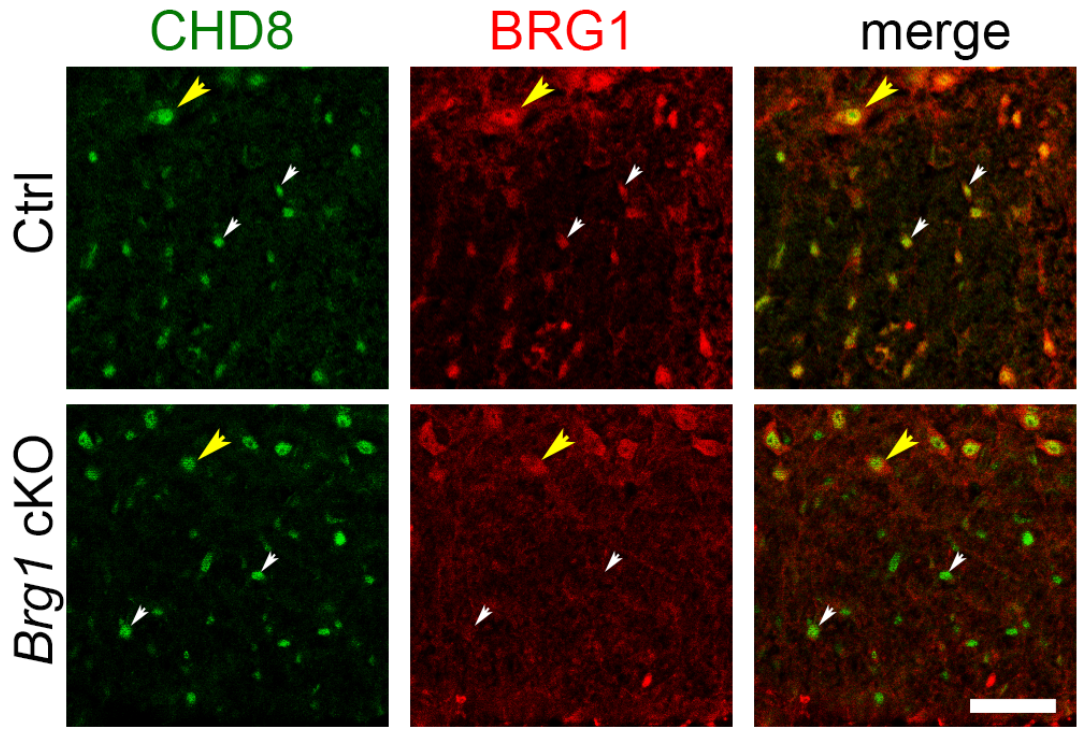

Figure S1. BRG1 and CHD8 expression in the spinal cord of *Brg1* cKO mice. Related to Figure 1.

The spinal cord sections of control and *Brg1* cKO mice at P7 were stained with BRG1 and CHD8. Scale bar, 50 μm.

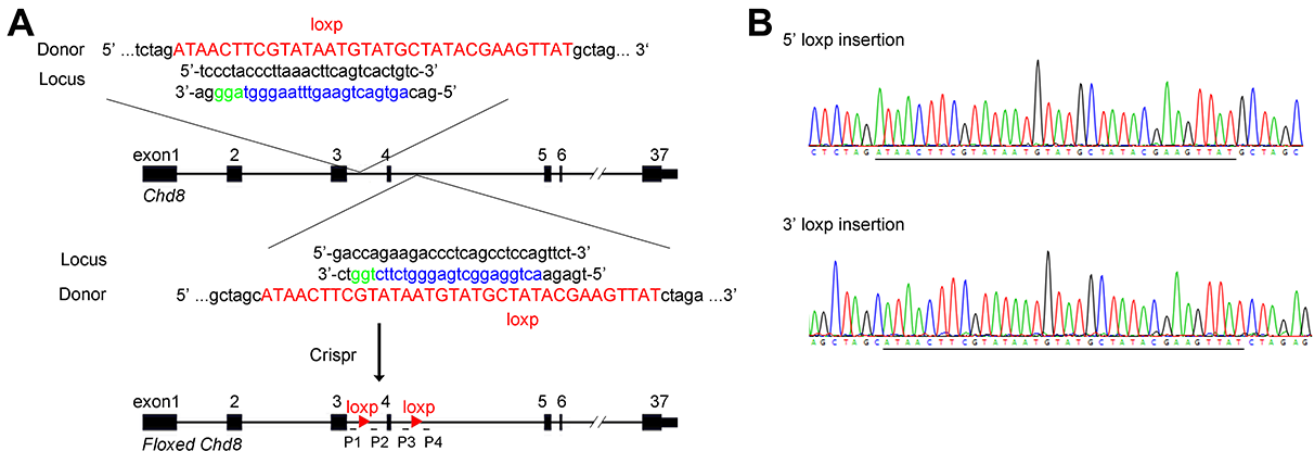

Figure S2. Generation and validation of mice carrying floxed *Chd8* alleles. Related to Figure 2.

A) Diagram depicting generation of *Chd8* allele with floxed exon 4 with CRISPR-Cas9 method.

B) Chromatogram of Sanger sequencing validation of loxp site insertion flanking the exon 4 of *Chd8* in mouse genome.

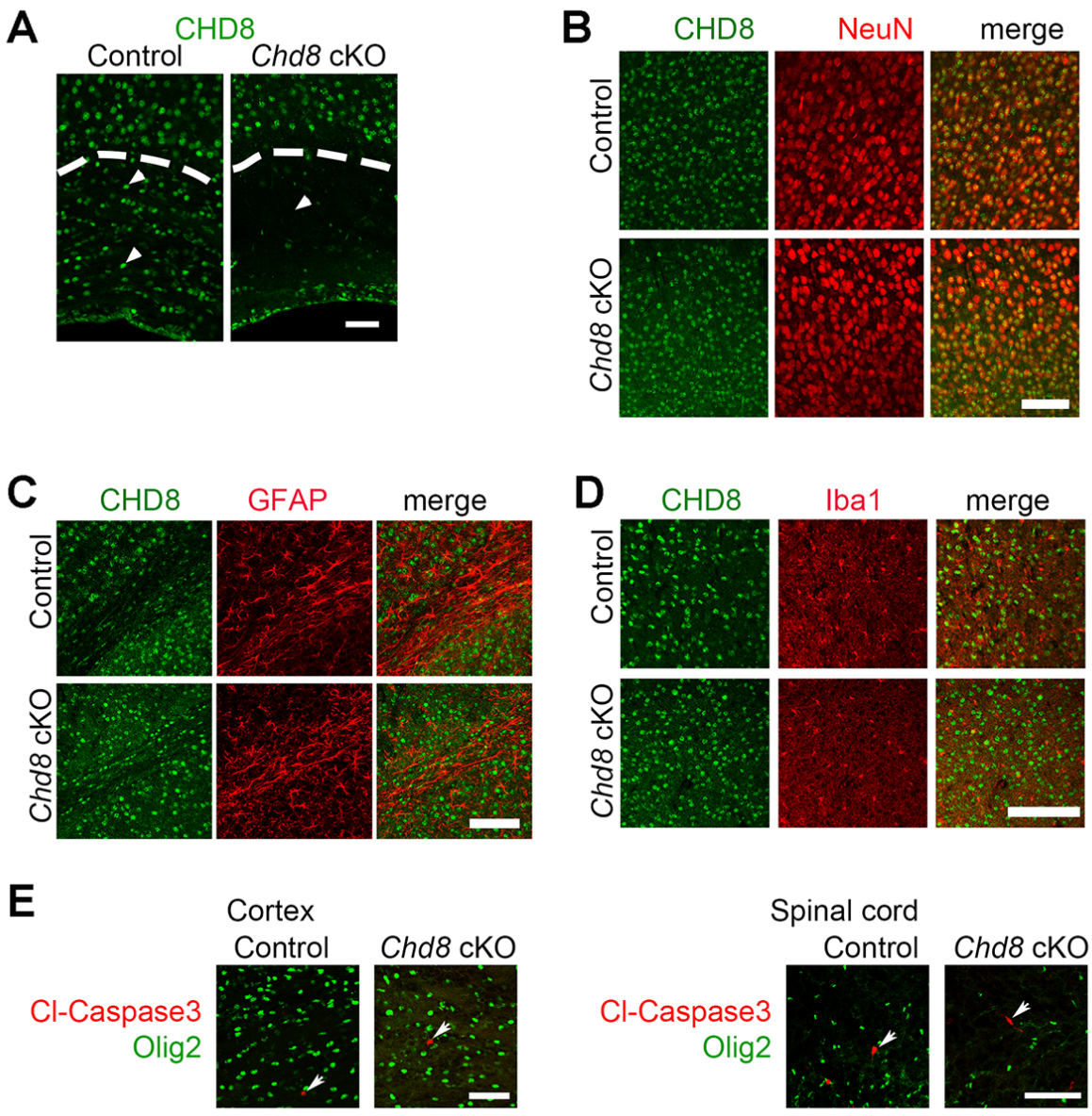

Figure S3. Extended analysis of *Chd8* cKO mice. Related to Figure 3.

A) The cortical sections of control and *Chd8* cKO mice at P14 were stained with CHD8. Scale bar, 100 μm.

B-D) The cortices of control and *Chd8* cKO mice at P14 were stained with the neuronal marker NeuN (B), astrocyte marker GFAP (C), microglia marker Iba1 (D). Scale bar, 100 μm.

E) The cortical and spinal cord sections of control and *Chd8* cKO mice at P1 were stained with Olig2 and an apoptotic cell marker, a cleaved form of caspase 3 (cl-caspase 3). Scale bar, 100 μm.

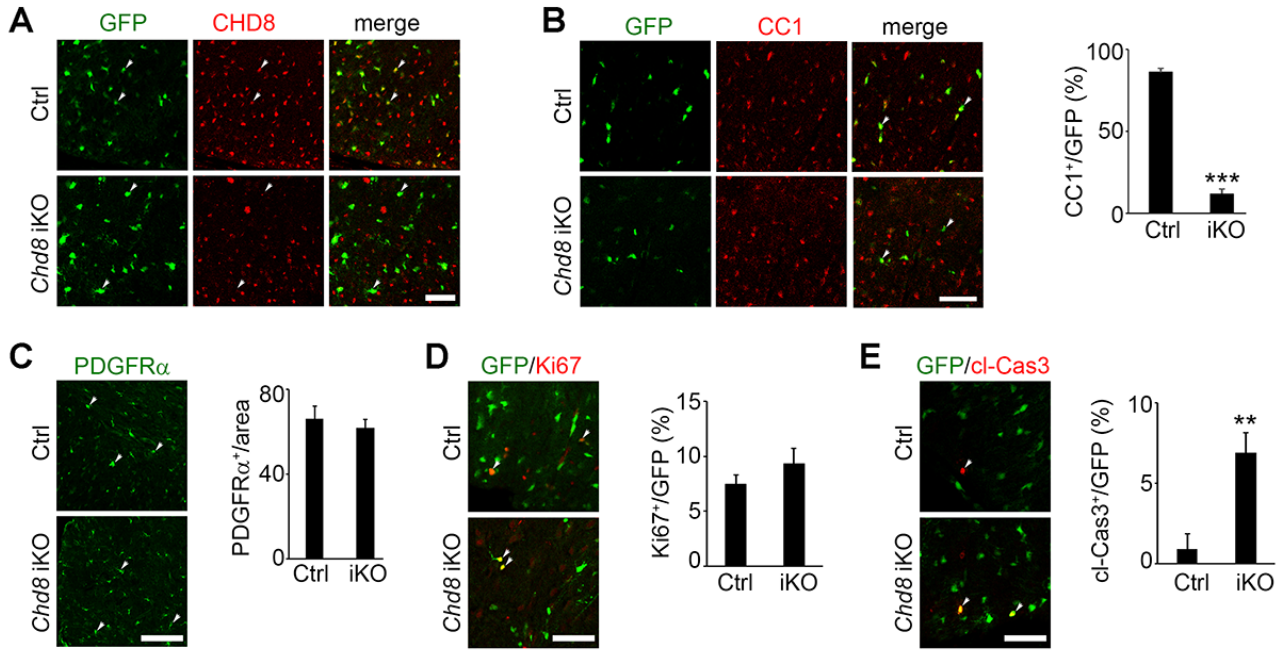

Figure S4. Inducible *Chd8* ablation in OPC cells impairs oligodendrocyte differentiation and survival but does not affect the OPC proliferation and number. Related to Figure 4.

A) The spinal cord of control and *Chd8* OPC-iKO mice at P14 were stained with CHD8. Scale bar, 50 μm.

B) Left, Immunostaining of CC1 on the spinal cord of control and *Chd8* OPC-iKO mice. Scale bar, 100 μm. Right, Quantification of $CC1^+$ oligodendrocyte cell numbers in the spinal cord of control and *Chd8* OPC-iKO mice at P14 (n = 4 independent experiments; *** $p < 0.001$, two-tailed unpaired Student's t test).

C) Left, Immunostaining of PDGFRα on the spinal cord of control and *Chd8* OPC-iKO mice. Scale bar, 100 μm. Right, Quantification of $PDGFR\alpha^+$ oligodendrocyte cell numbers in the spinal cord of control and *Chd8* OPC-iKO mice at P14.

D) Left, Immunostaining of Ki67 on the spinal cord of control and *Chd8* OPC-iKO mice. Scale bar, 100 μm. Right, Percentage of cleaved $Ki67^+$ cells among GFP^+ OPCs in the spinal cord of control and *Chd8* OPC-iKO mice at P14.

E) Left, Immunostaining of cleaved Caspase3 on the spinal cord of control and *Chd8* OPC-iKO mice. Scale bar, 100 μm. Right, Percentage of cleaved $Caspase3^+$ cells among GFP^+ OPCs in the

spinal cord of control and *Chd8* OPC-iKO mice at P14. (n = 4 independent experiments; *** $p < 0.001$, two-tailed unpaired Student's t test).

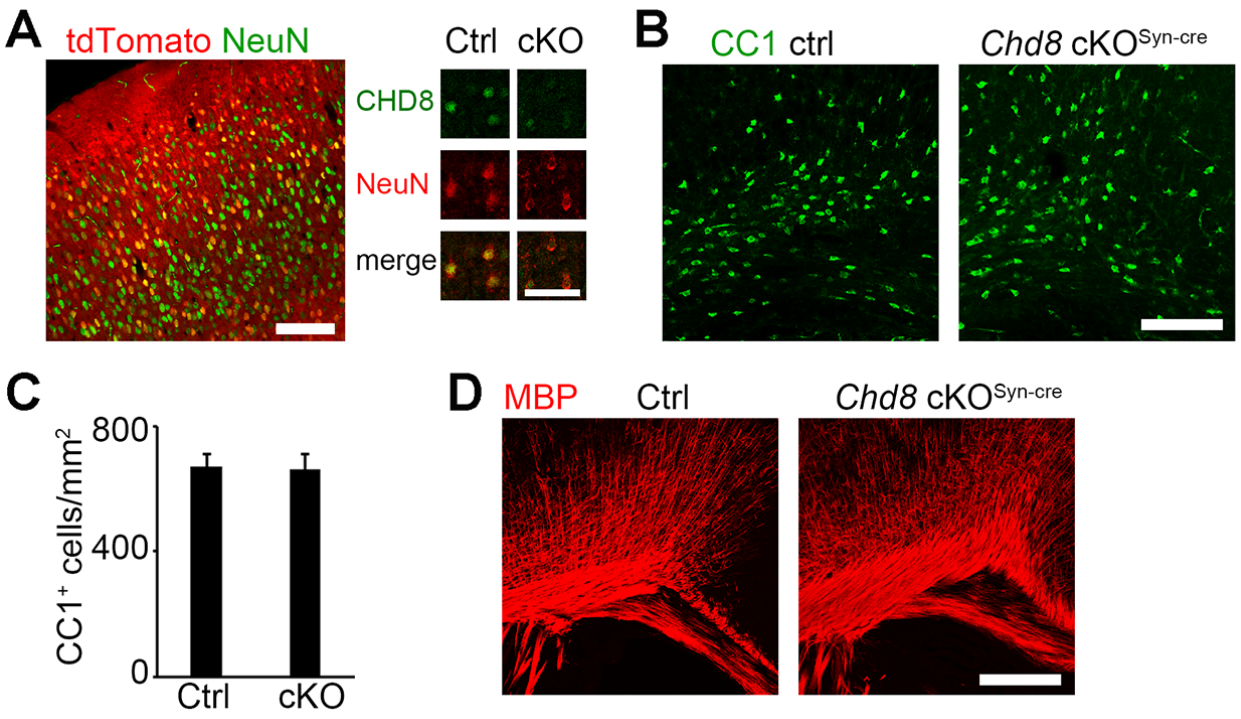

Figure S5. *Chd8* ablation in Synapsin1-Cre-expressing neurons does not impair oligodendrocyte differentiation. Related to Figure 4.

A) Left: tdTomato reporter expression in $NeuN^+$ neurons in the cortex of Synapsin1-Cre transgenic mice at P14. Scale bar, 100 μm. Right: Immunostaining of CHD8 and NeuN in the cortices of control and *Chd8* $cKO^{syn\text{-}cre}$ mice at P14. Scale bar, 50 μm.

B) Immunostaining of CC1 in the cortices of control and *Chd8* $cKO^{syn\text{-}cre}$ mice at P14. Scale bar, 100 μm.

C) Quantification of $CC1^+$ oligodendrocytes in the cortices of control and *Chd8* $cKO^{syn\text{-}cre}$ mice.

D) Immunostaining of MBP in the cortices of control and *Chd8* $cKO^{syn\text{-}cre}$ mice at P14. Scale bar, 100 μm.

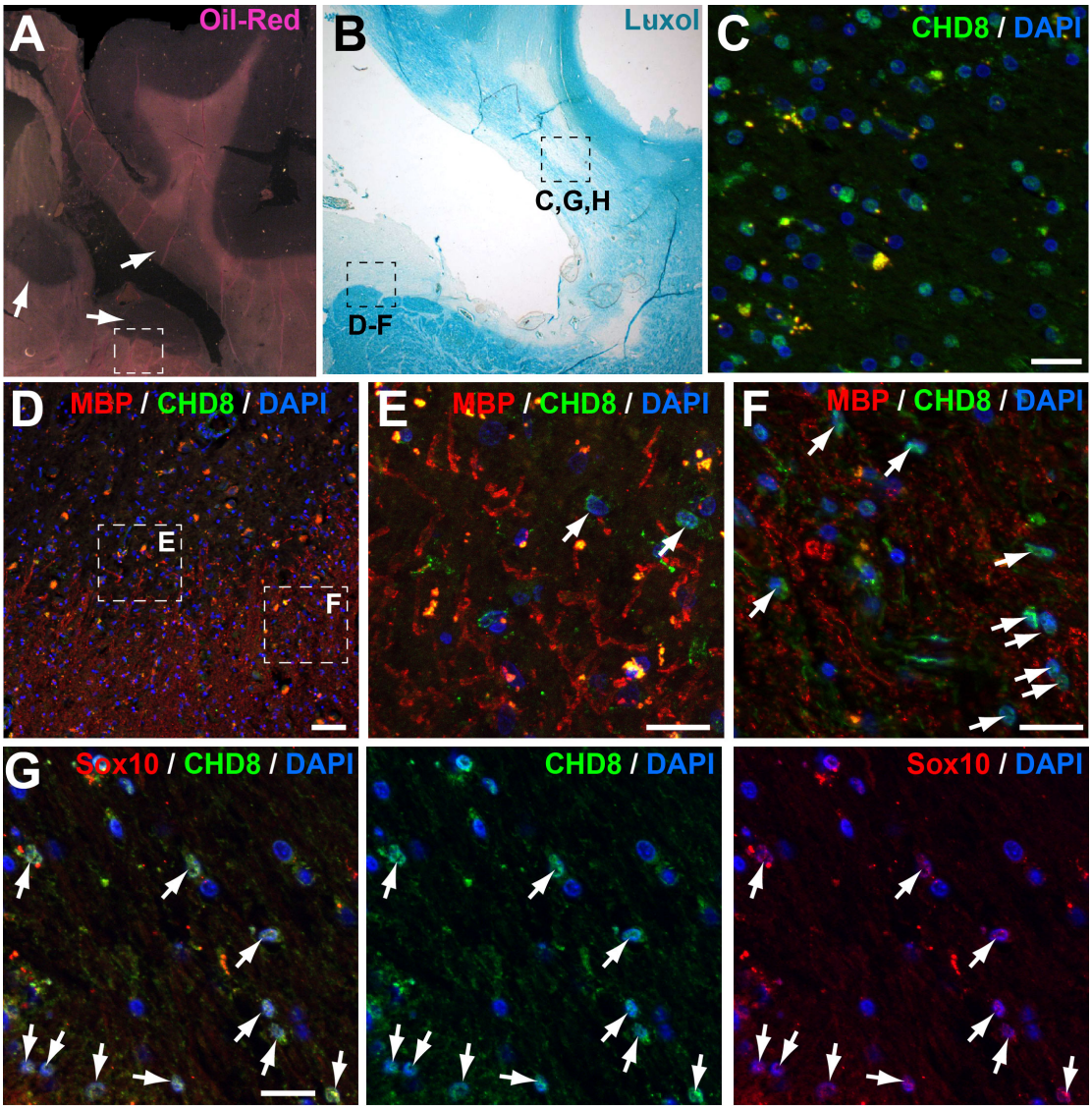

Figure S6. CHD8 expression in the brain lesion of multiple sclerosis patient tissues. Related to Figure 5.

A) Oil-Red staining showing white matter demyelinated areas as darker zones (arrows).

B) Luxol staining in adjacent section to tissue in (A) showing demyelinated areas (light blue staining). Insets indicated areas used in immunofluorescence staining following panels.

C) Demyelinated white matter track showing many small nuclei expressing CHD8 with typical oligodendrocytes alignments. Scale bars, 50 μm for panels C-G.

D) MBP staining showing the border area of re- and demyelination.

E, F) High magnification showing $CHD8^+$ nuclei (arrows) in remyelinating areas. Arrows show $CHD8^+$ cells.

G) High magnification picture showing that $CHD8^+$ cells are labelled by an anti-Sox10 antibody (arrows).

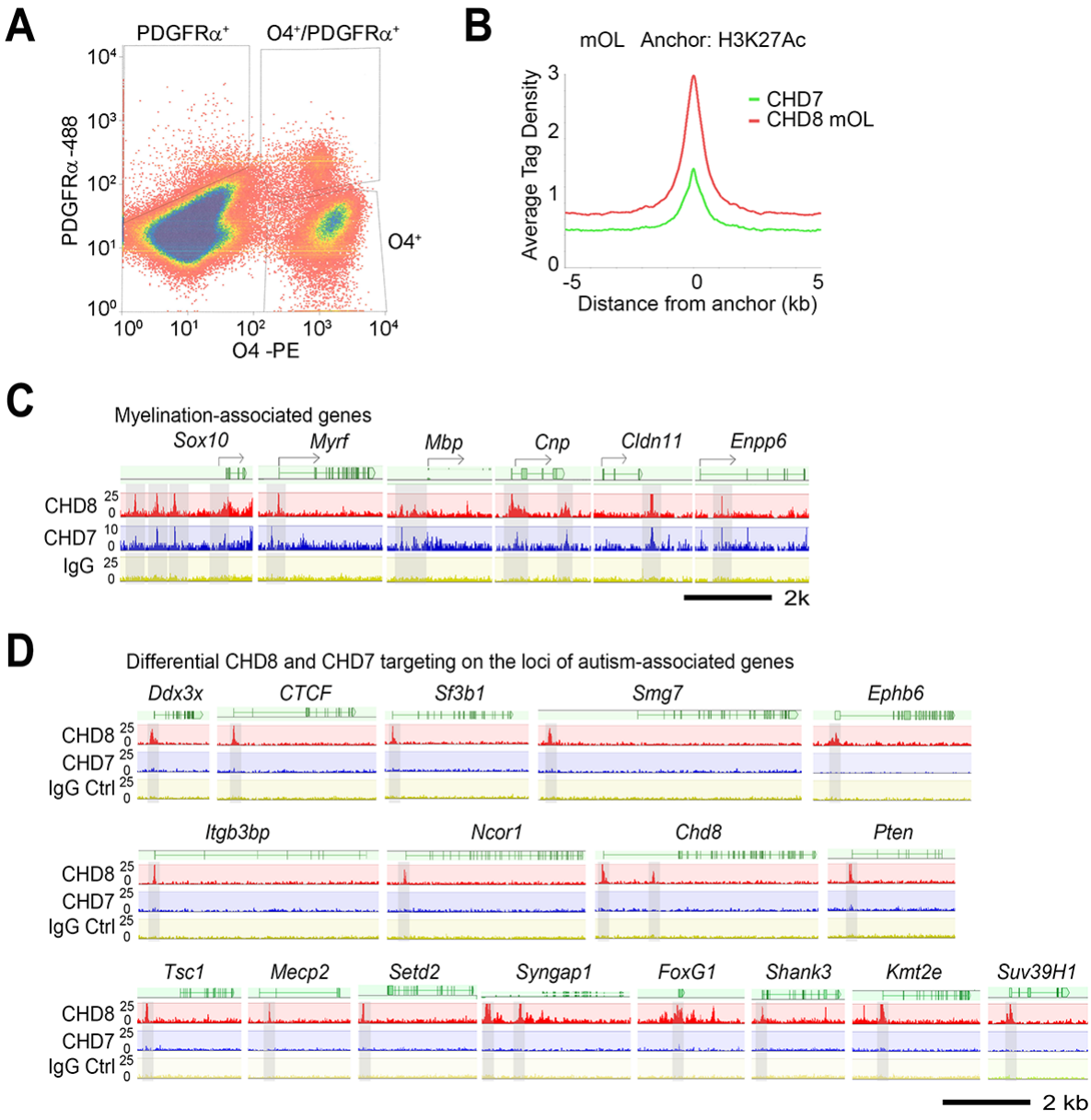

Figure S7. Comparison of CHD8 and CHD7 targeting to myelin-associated genes and autism-associated genes. Related to Figure 6.

A) Graph of FACS plots showing PDGFRα versus O4 expression intensity for isolating PDGFRα$^+$/O4$^+$ cells from control and *Chd8* cKO mouse cortices at P7.

B) The signal density of CHD8 and CHD7 peaks are plotted relative to H3K27Ac peaks in mOL.

C) Representative tracks of myelin-associated genes bound by CHD8 and CHD7 in mOL.

D) Representative tracks of autism-associated genes targeted by CHD8 and CHD7 in OPCs.

Supplemental Movies

Movie S1. *Chd8*-cKO mice exhibited tremors at P14. Related to Figure 2.

Movie S2. *Chd8*-cKO mice developed tonic seizures at P18. Related to Figure 2.